Holographic recording with reduced intermodulation noise in periodically poled lithium niobate

M. Werner and Th. Woike

Institut für Mineralogie und Geochemie, Universität zu Köln, Zülpicher Strasse 49b, D-50674 Köln, Germany

M. Imlau

Fachbereich Physik, Universität Osnabrück, Barbarastrasse 7, D-49069 Osnabrück, Germany

S. Odoulov

Institute of Physics, National Academy of Sciences, 03650, Kiev-39, Ukraine

Received August 11, 2004

We show that the use of periodically poled lithium niobate doped with Fe and Y ensures a considerable improvement in the quality of reconstructed images compared with the use of single-domain crystals. This improvement is due to inhibition of intermodulation noise and elimination of optical damage. © 2005 Optical Society of America

OCIS codes: 190.5330, 090.2900, 090.7330.

Crystals of Fe-doped lithium niobate ($LiNbO_3$) are considered a promising storage medium for holographic data storage, as was demonstrated in 1975.[1] They ensure a long dark storage time of several hundred years, high optical quality, and thus a considerably low bit-error rate of $\approx 3 \times 10^{-6}$, a large $M\#, \gg 1$, and acceptable sensitivity (see, e.g., Ref. 2 and the references therein).

At the same time the strong photorefractive nonlinearity of $LiNbO_3$, which is due to photovoltaic charge transport,[3] results not only in efficient hologram recording but also in severe light-induced distortions of the laser wave front, known as optical damage.[4] Furthermore, the photorefractive response of $LiNbO_3$:Fe is nearly independent of the angle between the two recording waves, including the range of very small angles.[3] This gives rise to the problem of intermodulation noise[5] that is due to recording and readout of holographic gratings by different low-spatial-frequency components of the image beam itself. These two factors, optical damage and intermodulation noise, degrade, to a certain extent, the performance of $LiNbO_3$ as a holographic recording medium.

Thus the ideal recording medium should be sensitive at high spatial frequencies, comparable to the carrier frequency of the hologram, and feature much smaller sensitivity at spatial frequencies of the image itself.[6] Periodically poled $LiNbO_3$ (PPLN) codoped with Fe and Y[7,8] meets these requirements, as follows from theoretical calculations.[9,10] An appropriate choice of the domain lattice spacing allows one to control the cutoff spatial frequency below which the nonlinear response of the material drops. We show in this letter that the use of PPLN diminishes intermodulation noise in reconstructed images and suppresses the appearance of ghost images even at rather high diffraction efficiencies of a hologram. Together with the known effects of inhibition of optical damage[7] and reduction of small-angle light-induced (nonlinear) scattering,[8] this ensures higher-quality reconstructed images than those obtained with single-domain crystals.

Bulk crystals with a periodic domain structure that spontaneously develops during growth were synthesized at Moscow University.[11,12] We use an x-cut sample (0.74-wt.% Y, 0.06-wt.% Fe) of 1-mm thickness with domain walls normal to the x axis and domain lattice period $L = 13$ μm. The sample offers a single-domain part (sd area) and a periodically poled part (pp area).[7,8]

To record the transmission holograms we use a holographic storage platform designed at the University of Cologne (partially described in Ref. 13). A frequency-doubled diode-pumped continuous-wave Nd^{3+}:YAG laser (single frequency, TEM_{00}, 150-mW output power, $\lambda = 532$ nm) is used for hologram re-

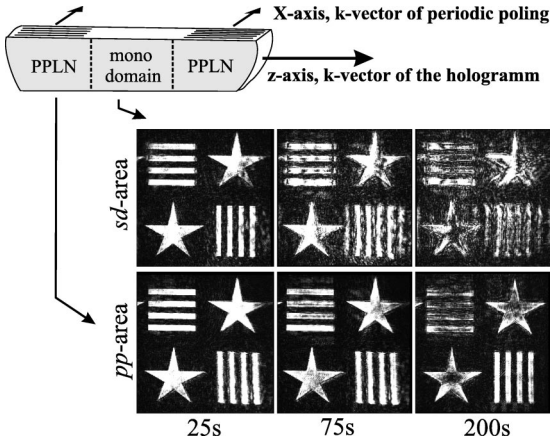

Fig. 1. Sample geometry of the $LiNbO_3$ sample and the holograms reconstructed from the sd and the pp areas for different exposure times.

0146-9592/05/060610-3/$15.00

cording. The laser light is polarized linearly, nearly along the z axis of the crystal and within the plane of beam intersection. The recording angle in air is $2\theta = 45°$. A schematic of the recording geometry is shown in Fig. 1.

A binary image is introduced into the object beam by a LCD page composer (1024×768 pixels). The signal-to-reference intensity ratio is 1:10. Holograms ~1-mm in diameter are recorded in front of the exact Fourier plane of the objective. The reconstructed images are captured by a CCD and stored with a PC.

Figure 1 also shows images reconstructed from holograms recorded in the sd and pp areas for various exposures. One can see that after 75-s exposure time the image from the sd area is already severely distorted. Note the appearance of ghost images (extra vertical bars and stars smeared horizontally) in the sd area, which is a typical manifestation of intermodulation noise. These effects are not visible for the pp area, where only a slight edge enhancement is observed for long exposures.

To analyze the reason for suppression of intermodulation noise in PPLN in more detail we study the photorefractive response of the crystal at typical spatial frequencies of the image from 10 to 100 mm^{-1}. For this purpose plane-wave holograms are recorded with the intensity ratio of the recording beams close to 1 by use of recording angles in the range 0.4°–12°. To monitor the grating recording as well as the appearance of higher orders of diffraction the diffraction patterns of an auxiliary He–Ne laser beam ($\lambda = 632.8$ nm) are analyzed. Figure 2 shows the angular intensity distribution of the red light in the far field for the sd and pp areas after 20 s of recording at angle $2\theta = 0.46°$.

In the ideal case, i.e., with no intermodulation effects, the diffraction orders would not be seen. Here the symmetric ±1 diffraction orders are obviously present, not only in the sd area but also in the pp area of the sample. Moreover, the second orders of diffraction are detectable, too. It should be pointed out that for $2\theta = 0.46°$ the 1-mm-thick grating can be considered to be thin already according to the Klein criterion, $Q = 2\pi\lambda l/n\Lambda^2 \simeq 0.4 \ll 10$, which explains the existence of higher orders of diffraction. From a comparison of the gray and black angular distributions it

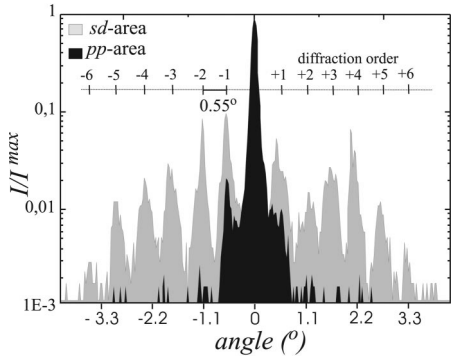

Fig. 2. Far-field intensity distribution for diffraction from the grating recorded in the sd and the pp areas for a recording angle of 0.46°.

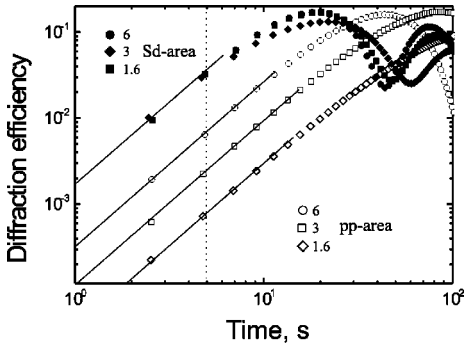

Fig. 3. Temporal evolution of the diffraction efficiency for $2\theta = 1.6°$ (diamonds), 3° (squares), and 6° (circles). Filled shapes, data for the sd area; open shapes, data for the pp area.

is obvious that the intensity of the diffracted beams in the pp area is much smaller than that in the sd area: the first-order peaks do not exceed a few percent in the pp area, whereas the second-order peaks are nearly invisible. This confirms that recording of holograms with spatial frequencies of the image, i.e., appearance of intermodulation noise, is inhibited in PPLN.

To get quantitative data we measure the diffraction efficiency η as a function of the grating spacing in the sd and pp areas. Instead of measuring the saturated values of η (that are masked by competing nonlinear effects, mainly by strong light-induced scattering) we measure η that is reached within a certain exposure time t that is much smaller than the grating decay time, $t \ll \tau$.

In Fig. 3 the temporal dynamics of the diffraction efficiency is shown for the sd and pp areas, measured at several recording angles with one of the recording green beams. In the following we select an exposure time $t = 5$ s for which the diffraction efficiency does not exceed a few percent, and where η increases $\propto t^2$. Thus the diffraction efficiency is proportional to the square of the ultimate space-charge field E_{sc}^{∞} that could be reached in the steady state, $\eta \propto (E_{sc}^{\infty})^2 (t/\tau)^2$ (see, e.g., Ref. 3). When we measure the kinetics of η at different recording angles, we see that at the beginning of recording all curves for the sd area are practically identical, whereas for the pp area the curves are all different: η decreases with increasing fringe spacing Λ. Thus, in accordance with our expectations, the space-charge field for the sd area, E_{sc}^{sd}, is nearly independent of the spatial frequency,[3] whereas that for the pp area E_{sc}^{pp} diminishes at low spatial frequencies.[9,10] It is useful to normalize the diffraction efficiency of the pp area, $\eta_{pp}(t)$, to the constant diffraction efficiency of the sd area, $\eta_{sd}(t)$, and evaluate from the experimental data the ratio of ultimate space-charge fields, $E_{sc}^{pp}/E_{sc}^{sd} = [\eta_{pp}(t)/\eta_{sd}(t)]^{1/2}$.

The dependence of the normalized space-charge field determined from the experimental data on the grating spacing for the sd and pp areas is shown in Fig. 4. In addition, the dashed curve refers to the relation[10]

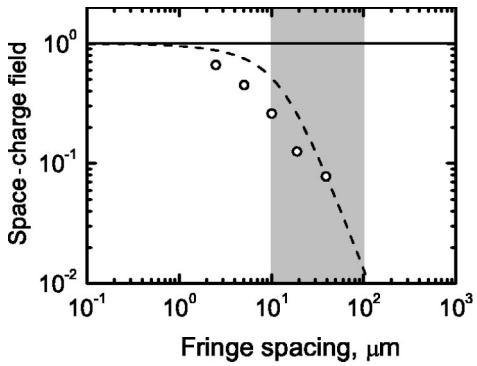

Fig. 4. Normalized space-charge field determined from the experimental data versus grating spacing for the pp area (open circles). Dashed curve and solid line, dependences calculated for domain lattice spacings of 13 μm (pp area) and ∞ (sd area), respectively. The gray field marks the range of image spatial frequencies.

$$\frac{E_{sc}^{pp}}{E_{sc}^{sd}} = 1 - \frac{2\Lambda}{\pi L}\tanh\left(\frac{\pi L}{2\Lambda}\right), \quad (1)$$

with domain lattice period $L = 13$ μm. The horizontal solid line, $E_{sc}/E_{sc}^{sd} = 1$, shows the expected behavior of a single-domain crystal, i.e., $L \to \infty$. A qualitative agreement of the measured and calculated data is evident despite the fact that the measured space-charge fields are roughly two times smaller than calculated. This may be a consequence of the imperfect domain periodicity as well as of accidental or Y-content-related topographic changes in sample sensitivity.

Starting from $\Lambda \geqslant 40$ μm, the measured data are strongly affected by the linear small-angle scattering of the readout beam from optical inhomogeneities of the sample. The low signal-to-noise ratio in this range leads to a linear (and not a quadratic) increase in the diffraction efficiency with time, so these data are not shown in Fig. 3. The presented data show that at $\Lambda = 10$ μm the amplitude of the space-charge grating is 4 times smaller than at $\Lambda \leqslant 1$ μm, typical for the hologram carrier frequency, whereas for $\Lambda = 40$ μm the difference becomes larger than 1 order of magnitude. Figure 4 permits extrapolation of the space-charge amplitude for a typical laser beam waist. For an unfocused laser beam of $\sim$1 mm the photorefractive response is inhibited by 4 orders of magnitude. This means that optical damage is eliminated in this medium, in full agreement with the conclusion of Ref. 7.

The sample that is used in this experiment is not optimized for intermodulation noise suppression. Much stronger suppression can be predicted with smaller domain lattice periods, e.g., for technologically accessible domain lattice period $L = 7$ μm.[7]

To conclude, substantial suppression of intermodulation noise has been demonstrated with image hologram recording in PPLN:Y:Fe crystals. As a result, holograms can be recorded even with strong overexposure, without quality losses of the image. This is of special importance for achieving high $M\#$ in holographic data storage. The suppression of intermodulation noise and optical damage in PPLN:Y:Fe should improve considerably the bit-error rate of $LiNbO_3$-based optical memories. However, to check this prediction bulk PPLN samples of larger dimensions are necessary.

We dedicate this article to the 65th anniversary of Eckhard Krätzig, who created in the Philips Research Laboratories one of the first photorefractive memories in the early 1970s. This work was supported in part by an Alexander von Humboldt Stiftung via a Research Award to S. Odoulov. We are grateful to Inna Naumova (Moscow State University) for the PPLN samples. M. Werner's e-mail address is marcus.werner@holozone.de

References

1. D. L. Staebler, W. J. Burke, W. Phillips, and J. J. Amodei, Appl. Phys. Lett. **26**, 182 (1975).
2. G. T. Sincerbox, in *Holographic Data Storage*, J. H. Coufal, ed. (Springer-Verlag, Berlin, 2000), pp. 3–59.
3. B. I. Sturman and V. M. Fridkin, *Photovoltaic and Photorefractive Effects in Noncentrosymmetric Materials* (Gordon & Breach, Philadelphia, 1992).
4. A. Ashkin, G. D. Boyd, J. M. Dzedzich, R. G. Smith, A. A. Ballman, J. J. Levinstein, and K. Nassau, Appl. Phys. Lett. **9**, 72 (1966).
5. R. J. Collier, C. B. Burckhardt, and L. H. Lin, *Optical Holography* (Academic, New York, 1971).
6. R. M. Shelby, in *Holographic Data Storage*, J. H. Coufal, ed. (Springer-Verlag, Berlin, 2000), pp. 101–109.
7. S. Odoulov, T. Tarabrova, A. Shumelyuk, I. I. Naumova, and T. O. Chaplina, Phys. Rev. Lett. **84**, 3294 (2000).
8. M. Goulkov, S. Odoulov, I. Naumova, F. Agulló-López, G. Calvo, E. Podivilov, B. Sturman, and V. Pruneri, Phys. Rev. Lett. **86**, 4021 (2001).
9. M. Taya, M. C. Bashaw, and M. M. Fejer, Opt. Lett. **21**, 857 (1996).
10. B. Sturman, M. Aguilar, F. Agulló-López, V. Pruneri, and P. Kazansky, J. Opt. Soc. Am. B **14**, 2641 (1997).
11. I. Naumova, N. Evlanova, O. Gilko, S. Larishchev, J. Cryst. Growth **181**, 160 (1997).
12. I. Naumova, N. F. Evlanova, S. A. Blokhin, and S. V. Larischev, J. Cryst. Growth **187**, 102 (1998).
13. M. Imlau, T. Bieringer, S. Odoulov, and Th. Woike, in *Nanoelectronics and Information Technology*, R. Waser, ed. (Wiley-VCH, Berlin, 2003).